## *Articles*

# Investigations of Neurotrophic Inhibitors of FK506 Binding Protein via Monte Carlo Simulations

Michelle L. Lamb and William L. Jorgensen*

*Department of Chemistry, Yale University, New Haven, Connecticut 06520-8107*

The binding and solution-phase properties of six inhibitors of FK506 binding protein (FKBP12) were investigated using free energy perturbation techniques in Monte Carlo statistical mechanics simulations. These nonimmunosuppressive molecules are of current interest for their neurotrophic activity when bound to FKBP12 as well as for their potential as building blocks for chemical inducers of protein dimerization. Relative binding affinities were computed and analyzed for ligands differing by a phenyl ring, an external phenyl or pyridyl substituent, and a pipecolyl or prolyl ring. Such results are, in general, valuable for inhibitor optimization and, in the present case, bring into question some of the previously reported binding data.

## Introduction

The α-ketoamide functionality of the immunosuppressant natural product FK506 (Figure 1) is retained in many of the highest affinity ligands that have been developed to inhibit the rotamase (cis−trans peptidyl-prolyl isomerase, or PPIase) activity[1] of the FK506 binding protein (FKBP12, MW = 12 kDa).[2] Originally, interpretation of the crystal structure of FK506−FKBP12 led to the belief that the α-ketoamide mimics a twisted-amide transition state of peptide bond isomerization, although an endogenous substrate for FKBP12 had not been discovered. It was thought that blockage of the isomerase active site prevented modification of downstream proteins necessary for T-cell activation, and this was the source of the observed immunosuppression. A similar mechanism had been proposed for the activity of the undecapeptide cyclosporin A (CsA), which inhibits the PPIase cyclophilin, although neither the natural products nor the proteins are homologous. However, evidence that rotamase inhibition was not sufficient for immunosuppression soon began to mount.[3] Rapamycin (Figure 1), another fungal molecule structurally similar to FK506, inhibited FKBP12 but appeared to influence a later stage of the T-cell cycle. Schreiber and co-workers[4] made a significant contribution with the synthesis of a molecule which retained the FKBP12 binding domain of FK506 and rapamycin (pyranose ring, α-ketoamide, pipecolate ester, and cyclohexyleth(en)yl groups), but in which the macrocycle was contracted. This molecule was a rotamase inhibitor but did not prevent T-cell proliferation.

It later became clear that the formation of an immunosuppressant−immunophilin complex results in a gain of function for the protein. The CsA−cyclophilin and FK506−FKBP12 pairs each present a recognition surface to the calcium-dependent, serine/threonine phosphatase, calcineurin (CN).[5] The FK506−FKBP12 complex binds at least 10 Å from the active site of CN and
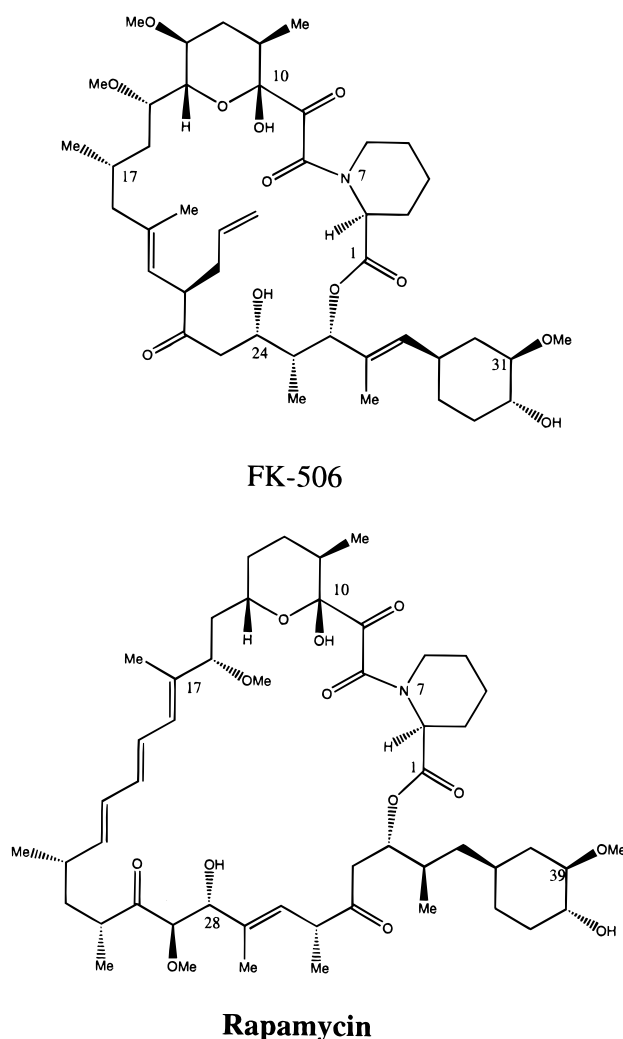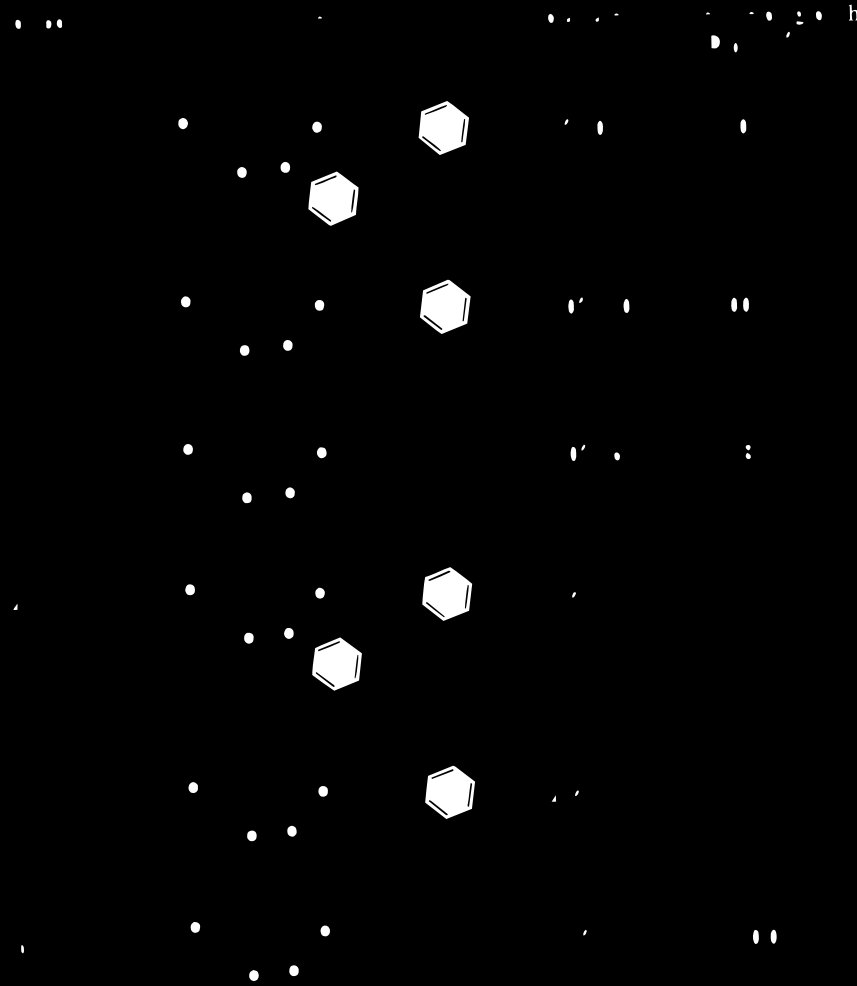


FK-506



**Rapamycin**

**Figure 1.** Structures and atom numbering for the immunosuppressants FK506 and rapamycin.

[a] Data on neurite outgrowth from chick dorsal root ganglia reported in ref 2. [b] Data from Guilford Pharmaceuticals, refs 2 and 59. [c] Data from SmithKline Beecham, refs 13 and 16.
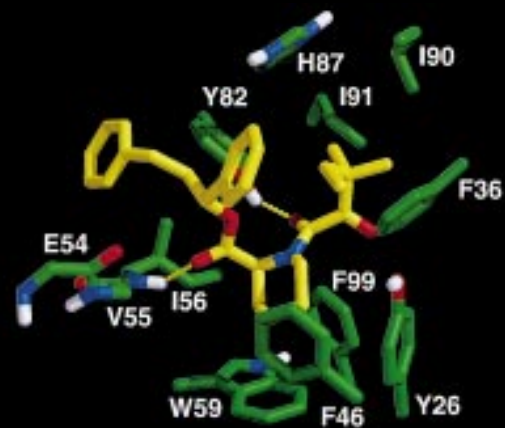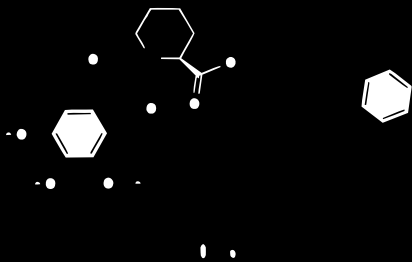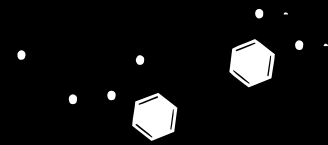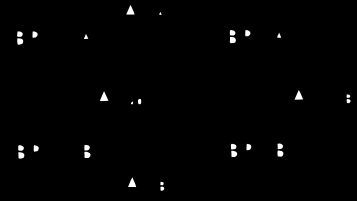


**Figure 2.** Position of compound **1** (yellow) in the aromatic binding pocket of FKBP12 (green).[13] Molecular graphics images were produced using the MidasPlus software system from the Computer Graphics Laboratory, University of California, San Francisco.[60]

**Scheme 1**

pipecolyl ring to prolyl are examined. There are discrepancies in the binding data from the two experimental sources, as indicated by the results for **2** and **3** in Table 1. From the crystal structure for **1** bound (Figure 2), the pyridine nitrogen of **3** is anticipated to be solvent exposed. Thus, it would normally not be expected to favor the lower dielectric environment of a protein ($\epsilon \approx$ 4) over that of bulk water ($\epsilon \approx 80$),[37] in contrast to the binding results from Guilford Pharmaceuticals. This was pursued through computations for the **2**, **3** and **5**, **6** pairs. Hamilton and Steiner have also pointed out that **5** and **6** are the first examples of prolyl compounds that bind better than their pipecolyl analogues, but the high affinity is attributed only to "improved design".[2] To investigate further, differences in free energies of binding were computed for two pairs of pipecolyl and prolyl ligands. Compounds **2** and **5** represent the unusual case with the prolyl ligand (**5**) as the better inhibitor. Compounds **1** and **4** represent the more common situation in which the presumably more hydrophobic pipecolyl ligand (**1**) has higher affinity for FKBP12.

## Computational Details

**Parametrization and Initial MC Simulations.** The crystal structure of **1**−FKBP12 at 2.0 Å resolution[13] from the Brookhaven Protein Data Bank[38] (entry 1fkg) was used as the starting point for the simulations. The computational protocol for the MC simulations was the same as in previous applications.[35,36] The good precision that is obtainable for free energy changes with this methodology was addressed extensively in ref 35. The MC sampling included variation of all bond angles and dihedrals of the ligand and protein side chains as well as overall rotation and translation of the ligand and water molecules. The protein backbone atoms were held fixed in their crystallographic positions. This makes the MC simulations more rapid, and the approximation is justified for FKBP12. Restricted backbone motion on the picosecond time scale has been noted for native FKBP12,[39] and ligand binding further rigidifies the protein structure, as demonstrated by the close resemblance among atomic structures of FKBP12 in numerous FKBP12−ligand complexes.[17] To be consistent with prior MD calculations on the FK506−FKBP12 system,[40] all 79 residues within 12 Å of FK506 in its cocrystal structure with FKBP12[14] were sampled. This provided a greater number of moving side chains than would be found in a 12 Å region around **1**.

The OPLS united-atom force field[41] with all-atom aromatic groups[42] provided most parameters for the protein; parameters for the inhibitors also came from this source and from a previous MD study of FK506.[43] A listing of parameters for the inhibitors is provided in the Supporting Information. The torsional parameters for the amino acid residues were derived from fitting to torsional energy profiles obtained from ab initio calculations with the 6-31G* basis set.[44] Any missing parameters were derived by fitting to MM2[45] energy profiles, which were generated using Macromodel.[46] A scale factor of $^1/_2$ was applied to all 1−4 nonbonded interactions. Histidines 25, 87, and 94 are known to be unprotonated,[47] and they were designated as $\partial$-tautomers based on visual inspection. This tautomeric state has

also been chosen in MD simulations of FKBP12−ligand complexes in solution.[32,34]

The unbound ligands and protein−ligand complexes were solvated with 22 Å spheres containing 1477 and 939 TIP4P water molecules, respectively. A half-harmonic potential with a 1.5 kcal/mol Å$^2$ force constant was employed to prevent waters from migrating away from the cluster. A 9 Å residue-based cutoff was used for all nonbonded interactions; if any pair of atoms from two residues was within this distance, all nonbonded interactions between the residues were included in the energy evaluation. The list of nonbonded interactions was updated every $2 \times 10^5$ configurations during the simulations.

All Monte Carlo simulations were performed with the MCPRO program.[48] An advantage of using internal coordinate MC methods is the ability to focus sampling on specific regions and degrees of freedom of interest. Consequently, bond lengths were fixed to their crystal structure values, and aromatic rings were treated as rigid units. To prevent inversion at sp$^3$ centers such as α-carbons and to enforce planarity of sp$^2$ centers for more efficient sampling, improper dihedral angles were not varied except as noted below. Otherwise, all bond angles and dihedrals in the moving portion of the system were sampled.

The MC simulations were carried out for 25 °C on Silicon Graphics workstations and on a cluster of personal computers using Pentium processors. It may be noted that the experimental results come from an assay for rotamase inhibition.[49] This widely used procedure for measuring FKBP12 binding affinities is usually performed somewhat below room temperature, e.g., near 10 °C.[13] The solvent was first sampled for 1 million (*M*) configurations to remove any highly repulsive initial contacts with the solutes. Then, 8*M* configurations were performed to equilibrate the **1**−FKBP12 complex. The same protocol was followed for **1** in solution, beginning with the bound conformation taken from the **1**−FKBP12 structure. During equilibration, the conformation of the bound ligand remained similar to the crystal conformation; however, partial inversion of the pipecolyl ring occurred in solution to switch it from a chair to a half-chair conformation (Figure 4). In gas-phase optimizations of ligand **1** with the present force field, the adopted ring conformation is favored by 1.3 kcal/mol. This is likely an artifact of using the AMBER C2−N−CH bending parameters with $\theta_0 = 118°$, which was not designed for a piperidine ring.[50] The difference is expected to have little effect on the computed free energy changes since the mutated phenyl rings are not in contact with the pipecolyl ring or, in the case of the ring contraction, the chair conformation was enforced (vide infra).

Free energy changes were calculated during the MC simulations according to standard procedures of statistical perturbation theory.[51−53] The difference in free energy of binding ($\Delta\Delta G_b$) for molecule B relative to molecule A (Scheme 1) may be obtained from transformations of the ligands in solution and bound to the protein according to eq 1:

$$\Delta\Delta G_b(A \rightarrow B) = \Delta G_B - \Delta G_A = \Delta G_{FKBP} - \Delta G_{aq} \quad (1)$$

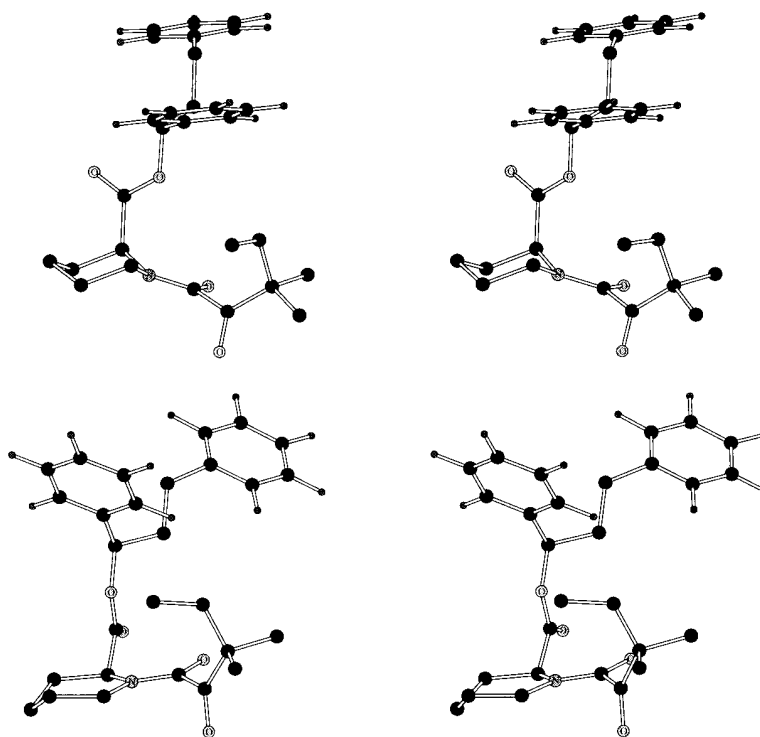**FEP Simulation Protocol for 1→2.** This perturba-

**Figure 4.** Stereoviews of unbound ligand **1**. The initial geometry from the **1**−FKBP12 crystal structure has the pipecolic ester substituent in an axial conformation (top). Subsequent equilibration resulted in partial inversion of the ring (bottom).

tion involved the removal of the 1-phenyl ring of **1** to obtain **2**. The atoms of the phenyl group were converted to "dummy" atoms without charge or Lennard-Jones parameters, and the length of the bond connecting the substituent to the remainder of the ligand was reduced to 0.65 Å with all other phenyl ring bonds reduced to 0.35 Å. The transformation of **1**→**2** was carried out in 13 windows with double-wide sampling, which yield 26 free energy increments.[51] A coupling parameter, $\lambda$, was employed such that $\lambda = 0$ corresponds to the initial state, **1**, and $\lambda = 1$ corresponds to the final state, **2**. The first six windows used $\Delta\lambda = \pm0.025$, while the remaining windows used $\Delta\lambda = \pm0.050$. All were equilibrated with $2-4M$ configurations of sampling; the last configuration of the previous window was used to start the next one. Averaging was done in batches of $2 \times 10^5$ configurations, with data collected over a total of $4-7M$ configurations in each window. For subsequent analyses of hydrogen bonding, an additional $1M$ configurations were generated at the endpoints of the simulations.

**FEP Simulation Protocol for 2→3, 5→6.** The next transformation addressed was the conversion of a phenyl moiety to a 3-pyridyl ring. This perturbation is straightforward; the analogous perturbation of benzene to pyridine had been performed in the development of OPLS all-atom (OPLS-AA) parameters for pyridine.[54] As before, the standard phenyl ring structure was transformed to a pyridine geometry determined from microwave experiments.[54] A model of **5** was required prior to the conversion of **5**→**6** and was obtained by mapping a prolyl ring onto the final structure of **2** from the **1**→**2** FEP calculation. In each simulation, the prolyl or pipecolyl ring was flexible. The perturbation protocol for these calculations was slightly modified from that

used for **1**→**2** to take advantage of the acquisition of a new parallel computing system within our laboratory. Seven double-wide windows were run in parallel, with $4-8M$ configurations sampled during the equilibration phase and with data collected over $4-12M$ configurations. A gas-phase FEP calculation was also performed for **5**→**6** to allow estimation of the relative free energies of hydration of the two ligands.

**FEP Simulation Protocol for 2→5, 1→4.** In our experience, perturbations between different cyclic systems require much care to implement and can be particularly slow to converge. The necessity of accounting for both changes in bonded and nonbonded interactions within the ring as one atom disappears makes this a technically difficult perturbation. One way to simplify the present calculations is to drive the ring from one fixed six-membered ring conformation to a fixed five-membered ring conformation, "disappearing" the remaining atom and simultaneously reeling it in toward the others. For this rigid perturbation, changes in energy within the ring need not be monitored, as these intraligand differences should be very similar in each environment (bound and unbound). However, other possible conformations for the rings would not be taken into account, and the results could be sensitive to the path chosen.

The simulations for the unbound and bound transformations were started from the final *bound* conformations of **2**−FKBP12 or **1**−FKBP12 above with the chair conformation for the pipecolyl ring. The final prolyl ring geometry was obtained from a gas-phase optimization of the bound conformation of **2** with one ring atom converted to a dummy atom, as illustrated in Figure 5. Other than for the internal structures of the pipecolyl and prolyl rings, the sampling for the ligands included

# DOCKET ALARM

# Explore Litigation Insights

Docket Alarm provides insights to develop a more informed litigation strategy and the peace of mind of knowing you're on top of things.

## Real-Time Litigation Alerts

Keep your litigation team up-to-date with **real-time alerts** and advanced team management tools built for the enterprise, all while greatly reducing PACER spend.

Our comprehensive service means we can handle Federal, State, and Administrative courts across the country.

## Advanced Docket Research

With over 230 million records, Docket Alarm's cloud-native docket research platform finds what other services can't. Coverage includes Federal, State, plus PTAB, TTAB, ITC and NLRB decisions, all in one place.

Identify arguments that have been successful in the past with full text, pinpoint searching. Link to case law cited within any court document via Fastcase.

## Analytics At Your Fingertips

Learn what happened the last time a particular judge, opposing counsel or company faced cases similar to yours.

Advanced out-of-the-box PTAB and TTAB analytics are always at your fingertips.

## API

Docket Alarm offers a powerful API (application programming interface) to developers that want to integrate case filings into their apps.

### LAW FIRMS
Build custom dashboards for your attorneys and clients with live data direct from the court.

Automate many repetitive legal tasks like conflict checks, document management, and marketing.

### FINANCIAL INSTITUTIONS
Litigation and bankruptcy checks for companies and debtors.

### E-DISCOVERY AND LEGAL VENDORS
Sync your system to PACER to automate legal marketing.